ARTICLE IN PRESS

Journal of Non-Crystalline Solids xxx (xxxx) xxx–xxx

Contents lists available at ScienceDirect

Journal of Non-Crystalline Solids

journal homepage: www.elsevier.com/locate/jnoncrysol

Structures and magneto optical property of diamagnetic TiO_2-TeO_2-PbO-B_2O_3 glass

Qiuling Chen*, Meng Zhang, Hui Wang, Qingwei Wang, Qiuhua Ma, Jie Li

School of Material Sciences & . Engineering, Henan University of Technology, Zhengzhou 450007, Henan, China

ARTICLE INFO

Keywords:
Faraday rotation
TiO_2 doping
Diamagnetic glass
Magneto optical sensing

ABSTRACT

TiO_2 doped diamagnetic 50.8TeO_2-29.2PbO-(20 − x)B_2O_3: xTiO_2 (where x = 0, 2, 5, 10, 15 and 20mol% respectively) glasses were synthesized and characterized in terms of their glass forming, structure, spectra and Faraday rotation using a home-made optical bench. The doped TiO_2 not only decreased glass transition temperatures, but also increased refractive index, Vickers hardness (352 HV), optical cutoff wavelength (458 nm) and Faraday rotation (0.2043 min/G·cm) at 632.8 nm wavelength.

1. Introduction

Magneto optical (MO) technology based on Faraday Effect is interesting in photonics, bio-sensor, magnetic field and current technology [1–3]. Amongst magneto optical materials, compared with gadolinium gallium garnet/yttrium iron garnet crystals and paramagnetic glass with high concentrations rare-earth, diamagnetic glasses, even though has relative low Verdet constant, owns promising advantages such as temperature independent Faraday rotation and easy for waveguides process (i.e. in fiber form) [4–7].

Due to its high refractive index and small band gap (3–3.2 eV), TiO_2 is an appealing dopant to be used in silicate [8], flint [9], fluorophosphates [10], fluorosilicate [11–12] and nonlinear optical glasses (e.g. the TiO_2-Nb_2O_5-Na_2O-SiO_2) [13–16] for photo-catalytic [17–21], dielectric [22] photovoltaic [23] applications etc. According to these studies, TiO_2 can change glass network structure by introducing non-bridging oxygen and defect centers.

However, the magneto optical property of TiO_2 for MO applications has not been investigated. In fact, these features of TiO_2 are very attractive to diamagnetic glass.

Thanks to its high polarization, good network former TeO_2 based glass exhibits the required characteristics for development of efficient MO components [24–28]. Heavy metal oxide with empty d orbital, PbO is considered to improve the magneto optical response. Due to the big mass and high polarization of Pb^{2+} ions, PbO glass possesses small photon energy and large refractive index which ensures them interesting in photonics and MO devices [29–32]. B_2O_3 can help the TeO_2 and PbO to form a vitreous network [33–36].

TiO_2 inhibits structural changes of the polyhedral Te and maintains a continuous glass network [37–40]. Moreover, TiO_2 can increase the thermal stability of TeO_2-based glasses by replacing Te-O-Te linkages with more rigid Te-O-Ti ones [41–45].

In this paper, we investigated the Faraday rotation of TiO_2 doped diamagnetic glass on the basis of previous study [46–50]. The effect of TiO_2 on glass forming, thermal [51–52], mechanical, optical [53] and magneto optical properties [54] is studied in order to get enhanced performances for diamagnetic glass. The Verdet constant of this study was compared with published results from other diamagnetic glass [55–61].

2. Experiments

2.1. TiO_2 doped magneto optical glass fabrication

Glasses with different compositions were fabricated by melt-quenching method. Start chemical reagents (99.99% purity) were weighted in 20–30 g batches according to 50.8 TeO_2–29.2 PbO–(20 − x) B_2O_3–x TeO_2 (x = 0, 2, 5, 10, 15 and 20 mol%). The batches were melted at 900 °C for 1 h. The melts were casted onto a 200 °C preheated brass plate and were annealed 2 h at 300 °C followed with cutting and optical polishing (λ-Logitech).

2.2. Glass characterization

Thermal properties in terms of glass transition temperature (T_g) and crystallization temperature (T_x) were measured using differential scanning calorimetry (Perkin-Elmer DSC7). Density at room temperature was measured following the Archimedes' principle using water as

* Corresponding author.
E-mail address: qlchen2016@163.com (Q. Chen).

http://dx.doi.org/10.1016/j.jnoncrysol.2017.04.020
Received 6 February 2017; Received in revised form 18 April 2017; Accepted 21 April 2017

immersion liquid. The refractive index (n) at three wavelengths was obtained by prism coupling method (Metricon 2010). UV absorption spectra between 200 nm–800 nm (Varian Cary 500) were recorded. Absorption coefficient can be calculated by Eq. (1):

$$\alpha = \frac{\log(^{I_0}/_{I})}{z} = A/z \tag{1}$$

where α is the absorption coefficient, A is the absorbance obtained from UV spectra, z is the sample thickness. Fourier transform infrared spectra (FT-IR) measurements from 400 to 4000 cm^{-1} were carried out (Varian Cary 500). XRD (Philips X'Pert diffractometer) was used to scan the crystalline quality. The XPS spectra for powder samples were measured (ESCALAB MK II) for information about chemical nature and elemental binding in TiO_2 doped glasses. Raman spectra were recorded from 140 to 860 cm^{-1} to acquire information related with glass structure.

Vicker's hardness was tested using a 136° pyramidal diamond indenter at a weight load of 200 g. Vicker's hardness can be calculated through Eq. (2): where P is the applied load in Kg, and d is mean length diagonal of the indentation in mm.

$$HV = 1.854P/d^2 \tag{2}$$

The Verdet constant was measured by a home-made optical bench as shown in Fig. 1. The 633 nm polarizated laser was focused on glass in solenoid, the signal after analyzer can be collected using a photo detector (Ophir PD300). The Verdet constant can be obtained through Eq. (3), where θ is Faraday rotation angle, *V* is Verdet constant, B is magnetic field, l is sample length.

$$\theta = VBl \tag{3}$$

A pure silica (with a known Verdet constant in literature [32]) is used as the reference for the sake of accuracy, before each measurement, the magnetic field inside solenoid was measured using a magnetometer to ensure a homogenous magnetic field distribution.

3. Results and discussion

3.1. FT-IR spectra

The FT-IR spectra of glasses are displayed in Fig. 2. It can be seen that glass containing higher TiO_2 presents higher FT-IR transmission, this is due to the strongly ionic Ti—O bonds entered the network and introduced the coordination defects with non-bridging oxygen ions (Te—O—…Ti^{4+}…—O—Pb) [26]. FTIR spectra in Fig. 2 confirmed that incorporation of TiO_2 changed coordination state of tellurium atom from TeO_4 through TeO_{3+1} to TeO_3. Unfortunately, the vibrations of TeO_4 structural units are not detected due to overlapping with TiO_6 unit between 635 and 670 cm^{-1} [20].

Band locates at 3200 cm^{-1}–3600 cm^{-1} is assigned to be O—H absorption, since the glass is fabricated in the air. The peak at

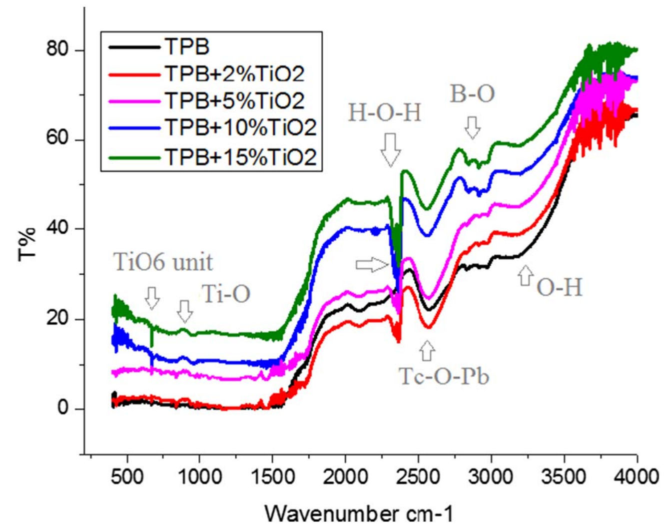

Fig. 2. FTIR spectra of TiO_2 doped TPB glasses between 400 and 4000 cm^{-1} wavenumber.

2360 cm^{-1} is resulted from the adsorbed H_2O molecules due to the optical property of TiO_2.

With TiO_2 increasing, the vibration of B—O bonds of $[BO_4]$ at 951 cm^{-1} and of $[BO_3]$ at 2800–3000 cm^{-1} became weaker, while the latter is stronger than the former, this indicates the $[BO_4]$ ➔ $[BO_3]$ units transition.

The TeO_2 and PbO contents were kept constant for all glasses, so the band of Te—O—Pb didn't change much around 2600 cm^{-1}.

The asymmetric vibrations of $[TiO_6]$ octahedron appeared at 650–700 cm^{-1} [16] which can be seen clearly in Fig. 3. It can be seen that vibration of Ti—O bonds becomes stronger for higher TiO_2 content. TiO_6 structural units band due to Ti-O-Ti vibration grown gradually and shift towards lower energies from 673 cm^{-1} to 663 $cm^{-1}$for 2% to 15% Ti, respectively. Similar result was reported on TiO_2 doped soda-lime-silicate glass [50]. In Fig. 3, Ti—O bonds vibrating around 910 cm^{-1} became stronger and broader with TiO_2 increasing indicating the $[TiO_4]$ ➔ $[TiO_6]$ transition [32]. Then paramagnetic Ti^{3+} occurs.

3.2. Glass forming

The glass forming appearance is listed in Table 1. There are some factors influence the glass forming: composition, quenching rate and the presence of impurities acting as nucleation centers [17]. During glass quenching from the liquid state, there are slow crystalline-like structure groups which continuously breaking up and reforming in the

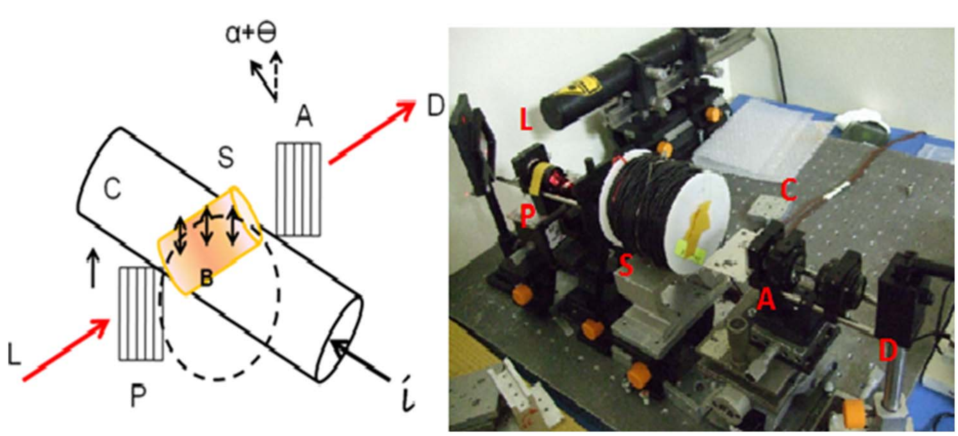

Fig. 1. Schematically setup for Verdet constant measurement of glass, L. He-Ne laser, P. polarizer, S. solenoid, C. current supplier, A. analyzer, D. detector.